Anal. Chem. **1995**, *67*, 2849–2857

Real-Time Detection of Single Molecules in Solution by Confocal Fluorescence Microscopy

Shuming Nie,† Daniel T. Chiu, and Richard N. Zare*

Department of Chemistry, Stanford University, Stanford, California 94305

We report real-time detection of single fluorescent molecules in solution with a simple technique that combines confocal microscopy, diffraction-limited laser excitation, and a high-efficiency photon detector. The probe volume, $\sim 5.0 \times 10^{-16}$ L, is defined latitudinally by optical diffraction and longitudinally by spherical aberration. With an unlimited excitation throughput and a low background level, this technique allows fluorescence detection of single rhodamine molecules with a signal-to-noise ratio of ~10 in 1 ms, which approaches the theoretical limit set by fluorescence saturation. Real-time measurements at a speed of 500 000 data points/s yield single-molecule fluorescence records that not only show the actual transit time of a particular molecule across the probe volume but also contain characteristically long (~50 μs) and short (~4 μs) dark gaps. Random-walk simulations of single fluorescent molecules provide evidence that these long and short dark periods are caused mainly by boundary recrossing motions of a single molecule at the probe volume periphery and by intersystem crossing into and out of the dark triplet state. We have also extended the use of confocal fluorescence microscopy to study individual, fluorescently tagged biomolecules, including deoxynucleotides, single-stranded primers, and double-stranded DNA. The achieved sensitivity permits dynamic structural studies of individual λ-phage DNA molecules labeled with intercalating fluorescent dyes; the results reveal large-amplitude DNA structural fluctuations that occur on the millisecond time scale.

A single molecule in liquid samples can be detected by combining the high sensitivity of laser-induced fluorescence (LIF) and the spatial localization and imaging capabilities of optical microscopy. In this procedure, the target molecule in solution is irradiated by a beam of light tuned to some electronic absorption feature. Because of rapid internal-state relaxation in both the excited and ground states, an individual molecule repeatedly undergoes an absorption–emission fluorescence cycle. This process continues as long as the irradiated molecule remains in the field of view and is not quenched by crossing over into some dark state, such as a triplet state, or by irreversible photochemical reaction (photobleaching). The characteristic fluorescence from the single molecule signals its presence and permits its identification and real-time monitoring of its behavior. Single-molecule detection in this manner depends on the ability to sense molecular fluorescence and concomitantly reject interference from scattered light (Rayleigh, Raman) and from fluorescence that originates from impurities. Real-time fluorescence detection of a single molecule has recently been made possible by two important advances. The use of confocal microscopy reduces the depth of field to 1 μm or less,[1] which leads to a sampling volume of subfemtoliters (less than 10^{-15} L). The use of supersensitive solid-state photon detectors, such as a single-photon avalanche diode (SPAD),[2] provides a quantum efficiency of more than 70% and a dark count of less than 10 counts/s. As Li and Davis[3] pointed out, this device may become the preferred one for detecting ultralow light levels when the light being measured can be focused to a small spot.

Rotman[4] was perhaps the first to use fluorescence detection for single-molecule studies in solution. Using a fluorogenic substrate, he measured in 1961 the presence of a single β-D-galactosidase molecule by detecting the fluorescent product molecules accumulated in a microdroplet through enzymatic amplification. This early work did not achieve single-molecule sensitivity but showed fluorescence detection of the product molecules generated by a single enzyme molecule. In 1976, Hirschfeld[5] reported the use of fluorescence microscopy to detect single antibody molecules tagged with 80–100 fluorescein molecules under evanescent-wave excitation and photobleaching conditions. Using fluorescence photomicroscopy and digital video microscopy, Webb and co-workers[6] later demonstrated detection and tracking of individual low-density lipoprotein particles, each containing an average of ~36 molecules of the highly fluorescent lipid analog dioctadecylindocarbocyanine (DiI-3). Similarly, Georgiou et al.[7] showed fluorescence monitoring of single influenza viruses labeled with ~100 octadecylrhodamine molecules. In fluorescence flow cytometry, Watson and Walport[8] achieved a detection limit of 730 labeled antibody–receptor complexes, equivalent to approximately 125–150 molecules of free fluorescein.

Keller and co-workers[9] first suggested the use of LIF for single-molecule detection in a flowing sample. Using a dual-

† Present address: Department of Chemistry, Indiana University, Bloomington, Indiana 47405.

(1) Pawley, J. B., Ed. *Handbook of Biological Confocal Microscopy*; Plenum Press: New York, 1990.
(2) Dautet, H.; Deschamps, P.; Dion, B.; MacGregor, A. D.; MacSween, D.; McIntyre, R. J.; Trottier, C.; Webb, P. P. *Appl. Opt.* **1993**, *32*, 3894–3900.
(3) Li, L.-Q.; Davis, L. M. *Rev. Sci. Instrum.* **1993**, *64*, 1524–1529.
(4) Rotman, B. *Proc. Natl. Acad. Sci. U.S.A.* **1961**, *47*, 1981–1991.
(5) Hirschfeld, T. *Appl. Opt.* **1976**, *15*, 2965–2966.
(6) Barak, L. S.; Webb, W. W. *J. Cell Biol.* **1981**, *90*, 595–604. Barak, L. S.; Webb, W. W. *J. Cell Biol.* **1982**, *95*, 846–852. Ghosh, R. N.; Webb, W. W. *Biophys. J.* **1994**, *66*, 1301–1318.
(7) Georgiou, G. N.; Morrison, I. E. G.; Cherry, R. J. *FEBS Lett.* **1989**, *250*, 487–492.
(8) Watson, J. V.; Walport, M. J. *J. Immunol. Methods* **1986**, *93*, 171–175.
(9) Dovichi, N. J.; Martin, J. C.; Jett, J. H.; Keller, R. A. *Science* **1982**, *219*, 845–847.

0003-2700/95/0367-2849$9.00/0

channel fluorescence detector, Dovichi and co-workers recently demonstrated the detection of six sulforhodamine molecules in a sheath-flow cuvette.[10] With flowing stream techniques, Nguyen and co-workers[11] and Peck and co-workers[12] showed single-molecule detection for the multichromophore protein β-phycoerythrin, which is equivalent to 25 rhodamine 6G (R6G) molecules in fluorescence. Using pulse laser excitation and time-gated fluorescence detection, Shera and co-workers[13] first detected individual single-chromophore molecules (R6G) in the liquid phase and later also with continuous-wave (CW) laser excitation.[14] The time-gated fluorescence technique recently has been extended to study mixtures of dye solutions,[15] to measure the lifetime of single rhodamine-101 molecules,[16,17] to detect individual near-IR dye molecules,[18] and to size single DNA molecules.[19] Ramsey and co-workers[20] also achieved single-molecule detection for R6G and phycoerythrin molecules in levitated microdroplets. Recently, Winefordner and co-workers[21] reported detection of single IR-140 dye molecules in a 11-μm-i.d. capillary by using a specially designed filter to reject scattered light in a narrow wavelength range.

Rigler and co-workers[22,23] first reported the use of a confocal microscope coupled with fluorescence correlation spectroscopy[24] to detect and study the translational diffusion of single R6G molecules in water. By reducing the probe volume to below a femtoliter (10^{-15} L), they could observe a large burst of fluorescence photons from a single molecule diffusing across the laser beam. This approach was recently employed for submillisecond detection[25] and triplet-state studies[26] of rhodamine molecules in solution. Eigen and Rigler[27] further suggested its application in molecular diagnostics and evolutionary biology. Fluorescence correlation spectroscopy measures intensity fluctuations over an observation period and analyzes the accumulated data statistically. The characteristic correlation time (τ_D) represents the statistical time for a molecule to diffuse out of a certain region and does not describe the behavior and dynamics of a particular molecule.[28]

In fluorescence correlation spectroscopy, the signal $S(t)$ at time t is correlated with itself (autocorrelation) at time $t + \tau$ to yield

$$G(\tau) = \lim_{T\to\infty} \frac{1}{T}\int_0^T S(t)S(t+\tau)\,dt \qquad (1)$$

The function $G(\tau)$ can be regarded to be the second moment of the displaced fluorescence signal, since $G(\tau) = \langle S^2 \rangle$ when $\tau = 0$ and $G(\tau) = \langle S \rangle^2$ when $\tau \to \infty$ where $\langle\ \rangle$ denotes average. Note that the form of the signal $S(t)$ cannot be recovered from $G(\tau)$ without knowledge of its functional dependence on time.

Using similar equipment, confocal microscopy, diffraction-limited laser excitation, and a somewhat improved model of a single-photon avalanche diode, we also reported single-molecule detection in room-temperature solutions but with sufficient signal to follow the fluorescence response of the single molecule without statistical or correlational analysis.[29] In this paper, we provide further details on real-time measurements of single dye molecules at a detection sensitivity that approaches the theoretical limit and we extend the use of confocal fluorescence microscopy to study individual biomolecules in buffer solution. Single-molecule fluorescence records obtained at 2-μs integration time show not only the actual transit time of a particular molecule across the probe volume but also characteristically long and short dark gaps. To understand the observed diffusional and photophysical behaviors of individual molecules in solution, we carried out simulation studies based on a random-walk model. The simulation results show that the long and short dark gaps are consistent with boundary recrossing motions of a single molecule at the probe volume periphery and intersystem crossing into and out of the dark triplet state. Through fluorescent labeling, we also report single-molecule detection for deoxynucleotides, single-stranded primers, and double-stranded DNA molecules. We show that the high sensitivity achieved allows real-time observation of DNA structural dynamics in free solution.

Because the equipment we used is inexpensive and readily available, we look forward to the routine application of real-time measurements of single molecules in solution. In particular, a rapid DNA sequencing scheme has been proposed by Keller and co-workers[30,31] based on the enzymatic cleavage of a fluorescently labeled DNA molecule and on-line detection of individual nucleotides being sequentially cleaved. Following a single molecule and chemical or biochemical reactions such a molecule may undergo can reveal new structural and dynamical features hidden in conventional measurements. Single-molecule techniques may also be used for ultrasensitive DNA analysis,[32] real-time monitoring of intracellular transport of biomolecules,[33] and rapid screening of rare molecules and nanostructures in large chemical libraries.[34]

The focus of this report is on the fluorescence detection of single molecules in ambient-temperature solutions. A related topic is single-molecule fluorescence detection in low-temperature

(10) Chen, D. Y.; Adelhelm, K.; Cheng, X. L.; Dovichi, N. J. *Analyst* **1994**, *119*, 349–352.
(11) Nguyen, D. C.; Keller, R. A.; Jett, J. H.; Martin, J. C. *Anal. Chem.* **1987**, *59*, 2158–2161.
(12) Peck, K.; Stryer, L.; Glazer, A. N.; Mathies, R. A. *Proc. Natl. Acad. Sci. U.S.A.* **1989**, *86*, 4087–4091.
(13) Shera, E. B.; Seitzinger, N. K.; Davis, L. M.; Keller, R. A.; Soper, S. A. *Chem. Phys. Lett.* **1990**, *174*, 553–557.
(14) Soper, S. A.; Shera, E. B.; Martin, J. C.; Jett, J. H.; Hahn, J. H.; Nutter, H. L.; Keller, R. A. *Anal. Chem.* **1991**, *63*, 432–437.
(15) Soper, S. A.; Davis, L. M.; Shera, E. B. *J. Opt. Soc. Am. B.* **1992**, *9*, 1761–1769.
(16) Tellinghuisen, J.; Goodwin, P. M.; Ambrose, W. P.; Martin, J. C.; Keller, R. A. *Anal. Chem.* **1994**, *66*, 64–72.
(17) Wilkerson, C. W.; Goodwin, P. W.; Ambrose, W. P.; Martin, J. C.; Keller, R. A. *Appl. Phys. Lett.* **1993**, *62*, 2030–2032.
(18) Soper, S. A.; Mattingly, Q. L.; Vegunta, P. *Anal. Chem.* **1993**, *65*, 740–747.
(19) Castro, A.; Fairfield, F. R.; Shera, E. B. *Anal. Chem.* **1993**, *65*, 849–852.
(20) Barnes, M. D.; Ng, K. C.; Whitten, W. B.; Ramsey, J. M. *Anal. Chem.* **1993**, *65*, 2360–2365.
(21) Lee, Y.-H.; Maus, R. G.; Smith, B. W.; Winefordner, J. D. *Anal. Chem.* **1994**, *66*, 4142–4149.
(22) Rigler, R.; Mets, U. *SPIE Proc.-Soc. Int. Opt. Eng.* **1992**, *1921*, 239–248.
(23) Rigler, R.; Mets, U.; Widengren, J.; Kask, P. *Eur. Biophys. J.* **1993**, *22*, 169–175.
(24) Magde, D.; Elson, E. L.; Webb, W. W. *Biopolymers* **1974**, *13*, 1–28, 29–61.
(25) Mets, U.; Rigler, R. *J. Fluoresc.* **1994**, *4*, 259–264.
(26) Widengren, J.; Rigler, R.; Mets, U. *J. Fluoresc.* **1994**, *4*, 255–258.
(27) Eigen, M.; Rigler, R. *Proc. Natl. Acad. Sci. U.S.A.* **1994**, *91*, 5740–5747.
(28) Berne, B. J.; Pecora, R. *Dynamic Light Scattering with Applications to Chemistry, Biology, and Physics*; Krieger: Malabar, FL, 1990.
(29) Nie, S.; Chiu, D. T.; Zare, R. N. *Science* **1994**, *266*, 1018–1021.
(30) Jett, J. H.; Keller, R. A.; Martin, J. C.; Marrone, B. L.; Moyviz, R. K.; Ratliff, R. L.; Seitzinger, N. K.; Shera, E. B.; Stewart, C. C. *J. Biomol. Struct. Dyn.* **1989**, *7*, 301–309.
(31) Soper, S. A.; Davis, L. M.; Fairfield, F. R.; Hammond, M. L.; Harger , C. A.; Jett, J. H.; Keller, R. A.; Marrone, B. L.; Martin, J. C.; Nutter, H. L.; Shera, E. B.; Simpson, D. J. *SPIE Proc.-Soc. Int. Opt. Eng.* **1991**, *1435*, 168–178.
(32) Hunkapiller, T.; Kaiser, R. J.; Koop, B. F.; Hood, L. *Science* **1991**, *254*, 59–67.
(33) Rothman, J. E. *Nature* **1994**, *372*, 55–63.
(34) Clackson, T.; Wells, J. A. *Trends Biotechnol.* **1994**, *12*, 173–184.

solids,[35-38] on silicon surfaces,[39] and through the use of near-field microscopy.[40-45] Several important differences should be noted, however. In ultra-low-temperature crystalline hosts, the single molecules being probed are dopants in a solid matrix, and detection is made possible by spectral isolation, but no spatial Brownian motion was present. In near-field optical microscopy, exceptional lateral resolution was achieved, ~12 nm,[44] but the close proximity of the metal-coated probe to the sample often causes perturbation of the probed molecule.[41,42] In addition, excitation power throughput is dramatically reduced (~50 nW for an 80-nm tip).[45]

EXPERIMENTAL SECTION

Apparatus. The confocal fluorescence microscopy system used for this work is described briefly elsewhere.[29] The apparatus consists of a Nikon Diaphot inverted microscope, a CW laser source focused to the diffraction limit, and a high-efficiency photodiode detector (Figure 1). Laser excitation at 488.0 and 514.5 nm was provided by an argon ion laser (Lexel Laser Inc., Fremont, CA). The laser beam entered the microscope through a back port and was directed to an oil immersion objective (100×, NA = 1.3, Nikon Instrument Group, Melville, NY) by a dichroic beam splitter (505DRLP02 or 540DRLP02, Omega Optical Inc., Brattleboro, VT). The laser beam was focused to a diffraction-limited spot by the high-NA objective, which was verified by comparing the laser focal size with 1-μm polystyrene microspheres (Duke Scientific, Palo Alto, CA). Fluorescence was collected by the same oil immersion objective and, after passing through the same dichroic beam splitter, was directed to a side port by a reflective mirror. Efficient rejection of out-of-focus signals was achieved by placing a precision pinhole (50–100-μm diameter, Newport Corp., Irving, CA) in the primary image plane. A single interference bandpass filter (Omega Optical Inc.) was used to reject the laser light and the Rayleigh- and Raman-scattered photons. The fluorescence signal was then focused on a photon-counting Si avalanche photodiode (Model SPCM-200, EG&G Canada, Vaudreuil, PQ, Canada), which provides a quantum efficiency of 55% at 630 nm and a dark noise of 7 counts/s.[2] The advantages of using an avalanche photodiode for single-molecule detection were first demonstrated by Li and Davis[3] in the time-gated detection mode. Both the pinhole and the photodiode detector were mounted on XYZ translation stages for ease of alignment. Time-dependent data were acquired by using a multichannel scalar (EG&G Ortec, Oak Ridge, TN) run on a personal computer (IBM PC-AT).

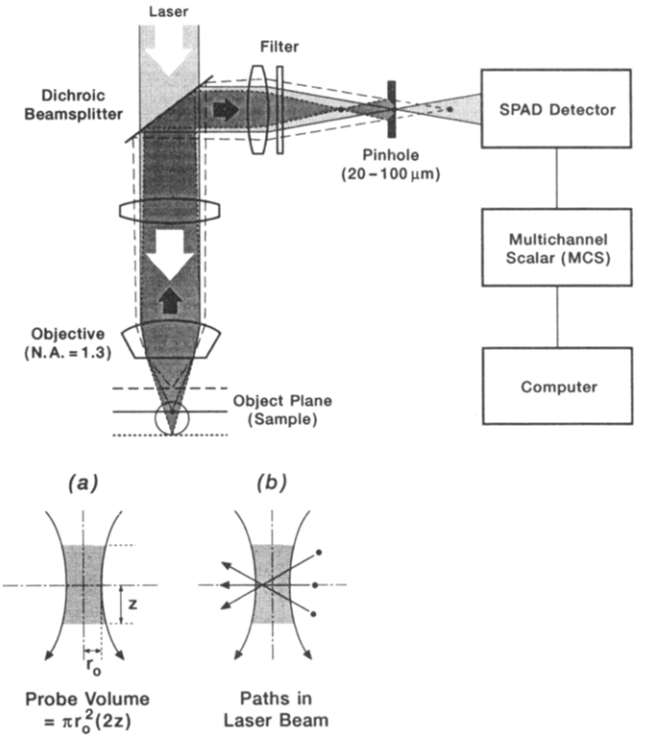

Figure 1. Schematic diagram of the confocal fluorescence microscopy system: (a) probe volume; (b) trajectories across the probe volume.

Procedures. Fluorescent labeling of DNA was carried out in TBE buffer (10 mM Tris, 10 mM borate, and 1 mM EDTA, pH 8) by adding a small volume of nucleic acid sample to an oxazole yellow homodimer (YOYO)[46,47] solution at a ratio of ~5 dyes/DNA molecule. This ratio has no particular biological significance in this study. After the mixture was kept for 30–45 min in the dark at room temperature, the sample was diluted to $\sim 10^{-9}$–10^{-10} M. To minimize sample decomposition, fresh dye solutions were prepared immediately before use by diluting the dimethoxy sulfoxide stock solution in TBE buffer.

To make fluorescence measurements, we pipeted an aliquot of the sample onto a clean cover glass (0.13-mm thick), and a larger glass slide was placed immediately on top to prevent solvent evaporation and to form a thin sample layer between the slides. The probe volume was continuously monitored at a speed ranging from 500 to 500 000 data points per second (2-ms to 2-μs integration) until detection events (bursts of photons) were observed. With a maximum capacity of 8192 data channels, each collection frame covered a time period of 16 s to 16 ms, depending on the specific data acquisition speed.

Reagents. The chemicals and biochemicals used in this work were obtained from commercial sources: fluorescein and rhodamine 6G perchlorate from Eastman Chemicals (Kingston, TN); fluorescein-12–2′-deoxyuridine 5′-triphosphate (fluorescein-12–dUTP) and tetramethylrhodamine-6–2′-deoxyuridine 5′-triphosphate (TMR-6–dUTP) from Boehringer Mannheim Corp. (Indianapolis, IN);

(35) Moerner, W. E. *Science* **1994**, *265*, 46–53.
(36) Orrit, M.; Bernard, J.; Personov, R. I. *J. Phys. Chem.* **1993**, *97*, 10256–10268.
(37) Moerner, W. E.; Pikhotnik, T.; Irngartinger, T.; Wild, U. P. *Phys. Rev. Lett.* **1994**, *73*, 2764–2767.
(38) Guttler, F.; Irngartinger, T.; Plakhotnik, T.; Renn, A.; Wild, U. P. *Chem. Phys. Lett.* **1994**, *217*, 393–397.
(39) Ishikawa, M.; Hirano, K.; Hayakawa, T.; Hosoi, S.; Brenner, S. *Jpn. J. Appl. Phys.* **1994**, *33*, 1571–1576.
(40) Trautman, J. K.; Macklin, J. J.; Brus, L. E.; Betzig, E. *Nature* **1994**, *369*, 40–42.
(41) Xie, X. S.; Dunn, R. C. *Science* **1994**, *265*, 361–364.
(42) Ambrose, W. P.; Goodwin, P. M.; Martin, J. V.; Keller, R. A. *Science* **1994**, *265*, 364–367.
(43) Betzig, E.; Chichester, R. J. *Science* **1993**, *262*, 1422–1425.
(44) Betzig, E.; Trautman, J. K.; Harris, T. D.; Weiner, J. S.; Kostelak, R. L. *Science* **1991**, *251*, 1468.
(45) Harris, T. D.; Grober, R. D.; Trautman, J. K.; Betzig, E. *Appl. Spectrosc.* **1994**, *48*, 14A–21A.
(46) Zhu, H.; Clark, S. M.; Benson, S. C.; Rye, H. S.; Glazer, A. N.; Mathies, R. A. *Anal. Chem.* **1994**, *66*, 1941–1948.
(47) Rye, H. S. Dabora, J. M.; Quesada, M. A.; Mathies, R. A.; Glazer, A. N. *Anal. Biochem.* **1993**, *208*, 144. Rye, H. S.; Yue, S.; Wemmer, D. E.; Quesada, M. A.; Haugland, R. P; Mathies, R. A.; Glazer, A. N. *Nucleic Acids Res.* **1992**, *20*, 2803–2812.

ultrapure EDTA, boric acid, Tris, and 2-mercaptoethanol (98+%) from Sigma Chemical Co. (St. Louis, MO); bacteriophage λ-DNA (48 502 bp) and pBR322 plasmid DNA (4363 bp) from New England Biolabs (Beverly, MA); 4,4-difluoro-4-bora-3a,4a-diaza-*s*-indacene (BODIPY-FL), tetramethylrhodamine–avidin conjugate, fluorescent microspheres (14 nm–1.0 μm in diameter), YOYO, and fluorescein-labeled and BODIPY FL-labeled M13/pUC primers from Molecular Probes (Eugene, OR); spectrophotometric grade ethanol and dimethylformamide (DMF) from Aldrich Chemical Co. (Milwaukee, WI). Water was purified with a Milli-Q purification system (Millipore, Bedford, MA). Stock solutions were prepared by dissolving the dyes in DMF, and the required concentrations were obtained by serial dilution of the stock solution in the appropriate solvent or buffer.

RESULTS AND DISCUSSION

Concentration Studies. In the absence of external forces, molecules are in constant random motion in solution. The probability of detecting a single target molecule depends on both the probe volume and its concentration. In confocal fluorescence microscopy, the probe (or sampling) volume is effectively an elongated cylinder (Figure 1), and its radius is determined by optical diffraction and its length by spherical aberration.[23,48] For a propagating Gaussian laser beam focused by a diffraction-limited objective, the $1/e^2$ radius at the focal plane is $r_0 = \lambda f/n\pi d_0$, where λ is the laser wavelength in vacuum, f is the focal length of the objective, n is the refractive index of the media (immersion oil $n = 1.52$), and d_0 is the $1/e^2$ radius of the input laser beam.[49] The diffraction-limited radius was calculated to be 250–260 nm under our experimental conditions (TEM_{00} laser beam radius 0.65 mm, objective focal length 1.6 mm, laser wavelength 488.0 or 514.5 nm). In theory, the $1/e^2$ probe depth (z) in confocal microscopy can be estimated by using the point spread function and collection efficiency function;[50] in practice, however, it is primarily determined by spherical aberration of the objective and has been experimentally measured to be ~1.0 μm.[23] The cylindrical probe volume is thus estimated to be $\sim 5.0 \times 10^{-16}$ L.

The tiny probe volume is expected to contain an average of only one dye molecule in a 3.3×10^{-9} M solution, but the actual number of molecules in it fluctuates between zero and one, one and two, etc. Poisson distribution predicts an equal probability (0.3679) for one or zero molecule in the probe volume and a lower probability (0.1839) for two molecules.[51] In more dilute solutions, the detection events are increasingly dominated by single molecules because the probabilities for two or more molecules in the probe volume become negligibly small. Figure 2 shows fluctuating fluorescence signals observed from a 1×10^{-9} and a 5×10^{-9} M R6G solution. The results demonstrate experimentally that the probe volume contains zero or one dye molecule and rarely two at a concentration of 1×10^{-9} M. Significant signal overlapping occurs at 5×10^{-9} M because the probe volume rarely becomes "empty". However, most "double occupancies" at 5×10^{-9} M are transient events; that is, the probe volume contains more than one molecule only transiently. The observed fluorescence peak

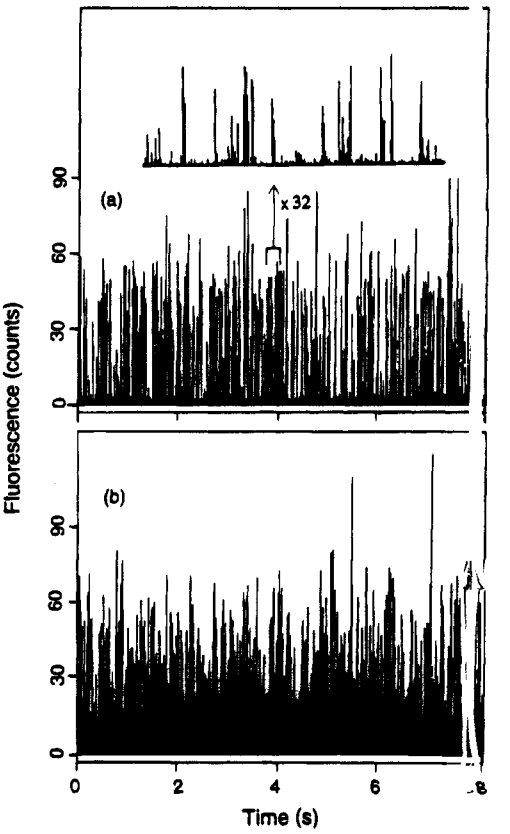

Figure 2. Fluctuating fluorescence signals observed from (a) 1×10^{-9} and (b) 5×10^{-9} M R6G. Data acquisition speed, 1000 data points/s (1-ms integration); CW laser excitation wavelength, 514.5 nm; laser power, 1 mW; emission bandpass filter, 560 nm (fwhm 40 nm). The inset is an expanded (×32) view of a small section of the data, showing discrete single-molecule signals.

intensities are only slightly higher because the effect of these transient "double-occupancy" events is averaged by signal integration. The dilution studies we carried out provide evidence that the observed fluorescence signals are truly single-molecule events and are not caused by molecular aggregates or artifacts such as dust scattering. Other criteria we used to ascertain single-molecule events include signal intensity dependence on the nature of solvent and pH and fluorescence saturation with increasing laser intensity.[29] For example, the fluorecence intensity of fluorescein-12–dUTP at pH 7 is much less than that at pH 12 (Figure 7), consistent with the pH-sensitive nature of fluorescein.

Single-Molecule Behavior. The achieved detection sensitivity allows real-time measurements of a single molecule in solution. To investigate the influence of solvent viscosity and analyte molecular weight, we studied the diffusional behavior of individual dye molecules and dye–protein conjugates in different solvents. Figure 3 shows fluorescence detection of single R6G molecules in ethanol and in ethanol–glycerol (1:1 v/v) as well as TMR–avidin conjugates in Tris buffer. As measured by the peak width, single-molecule transit times are significantly longer in the more viscous ethanol–glycerol solvent and for the heavier TMR–avidin conjugate in Tris buffer. This result is in qualitative agreement with the expected diffusion dependence on viscosity and molecular weight. As briefly noted previously,[29] a single molecule can be detected multiple times while moving in and out of the probe volume. Indeed, the observed signals tend to be doublets or

(48) Schneider, M. B.; Webb, W. W. *Appl. Opt.* **1981**, *20*, 1382–1388.
(49) Dickson, L. D. *Appl. Opt.* **1970**, *9*, 1854–1861.
(50) Qian, H.; Elson, E. L. *Appl. Opt.* **1991**, *30*, 1185.
(51) Feller, W. *An Introduction to Probability Theory and its Applications*, 3rd ed.; John Wiley and Sons: New York, 1968.

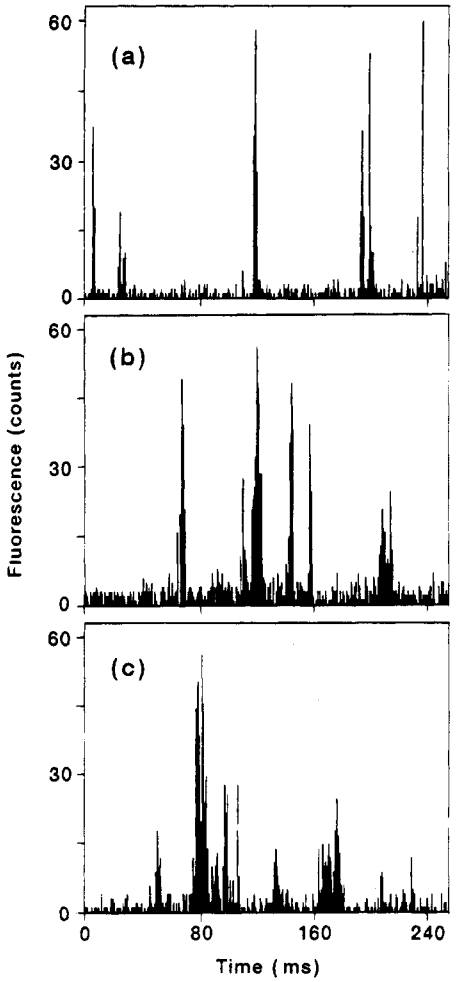

Figure 3. Fluorescence detection of individual R6G molecules and TMR–avidin conjugates in different sampling environments: (a) 5×10^{-11} M R6G in ethanol; (b) 2×10^{-10} M R6G in ethanol–glycerol (1:1); (c) 1×10^{-10} M TMR–avidin conjugate in aqueous 50 mM Tris buffer (pH 7). Laser wavelength, 514.5 nm; excitation power, 0.7 mW; emission bandpass filter, 560 nm (fwhm 40 nm); integration interval, 1.0 ms.

triplets, and the signal-clustering effect becomes more apparent in the more viscous solvent and for the heavier conjugate molecules because of the reduced diffusion coefficients. Approximately 2.6 dye molecules are attached to each TMR–avidin conjugate, but a particular avidin molecule may contain zero, one, two, or more fluorescent labels according to Poisson statistics.[51] Individual detection events presented in this study depend on the particular path (trajectory) of a particular molecule in the probe volume. Broad and intense fluorescence signals arise from molecules that carry multiple labels or spend long periods of time in the probe volume, whereas relatively weak signals indicate those that have fewer labels or follow shorter paths. We further note that after a large number of detection events have been accumulated, a histogram plot should show recognizable peaks, each corresponding to avidin proteins labeled with one, two, or more dye molecules.

In addition to transit time measurements on the millisecond time scale, we examined the diffusional and fluorescence behaviors of single molecules on the microsecond time scale at a recording speed of 500 000 data points/s. Figure 4 shows a fluorescence record observed from a single R6G molecule in

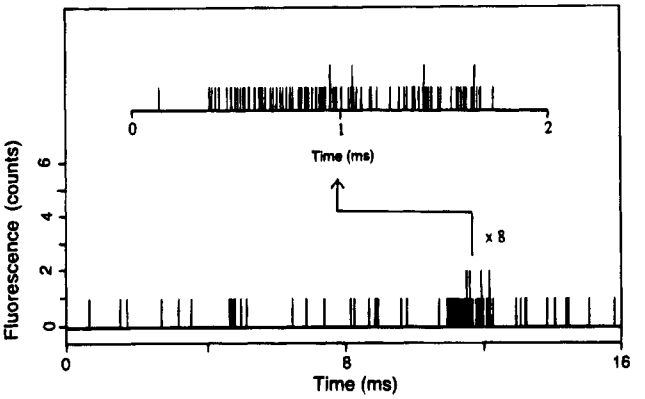

Figure 4. Fluorescence record of a single R6G molecule in ethanol obtained at 500 000 data points/s (2-μs integration) and a CW laser power of 1 mW (514.5 nm). Emission bandpass filter, 560 nm (40-nm fwhm).

ethanol. With 2-μs integration and ~1% detection efficiency, the fluorescence record consists of predominantly single-photon events with a time spread of ~1.2 ms, which corresponds to the actual transit time of that particular molecule and is considerably longer than the typical transit time of ~0.7 ms. Moreover, the observed "light trail" is not continuous but contains several long dark gaps of ~50 μs and numerous short dark gaps. The appearance of long dark periods indicates that a molecule in solution may recross the probe volume periphery several times before eventually diffusing away. When the molecule is temporarily out of the probe volume through such boundary excursions, no fluorescence photons are detected until it recrosses back into the probe volume. To account for the short dark gaps, which have an average duration not much longer than the data integration time (2 μs), we recognize that the exact temporal relationship between the observed and the true photon emission process is complicated by the fact that only ~1% of the emitted photons is detected. Nonetheless, the average elapsed time (~4–6 μs) between adjacent detected photons is only slightly longer than the triplet lifetime (4 μs) of R6G in aerated ethanol,[52,53] which indicates that intersystem crossing into and out of the triplet state plays a role in causing the short dark periods. With a calculated fluorescence cycle time of ~10 ns at 1.0-mW laser excitation (514.5 nm),[29] a R6G molecule is expected to emit 100 fluorescence photons in 1 μs, which leads to one detected photon count (~1% detection efficiency). On the average, for every 500 fluorescence cycles (or ~5 μs), the molecule crosses once into the triplet state (intersystem crossing efficiency ~0.2%).[53,54] Therefore, a triplet-caused dark gap occurs every 5 μs on the average and lasts an average time of ~4 μs. The involvement of the triplet state can thus cause alternating dark and bright periods that have an average duration of 4–6 μs.

Random-walk simulation studies we carried out[55] provide further evidence for the boundary recrossing motions of a single molecule and the triplet-state effect on fluorescence emission. Figure 5 shows the simulated diffusion path of a single R6G

(52) Thiel, E.; Drexhage, K. H. *Chem. Phys. Lett.* **1992**, *199*, 329–334.
(53) Asimov, M. M.; Gavrilenko, V. N.; Rubinov, A. N. *J. Lumin.* **1990**, *46*, 243–249.
(54) Dempster, D. N.; Morrow, T.; Quinn, M. F. *J. Photochem.* **1973**, *2*, 343–359.

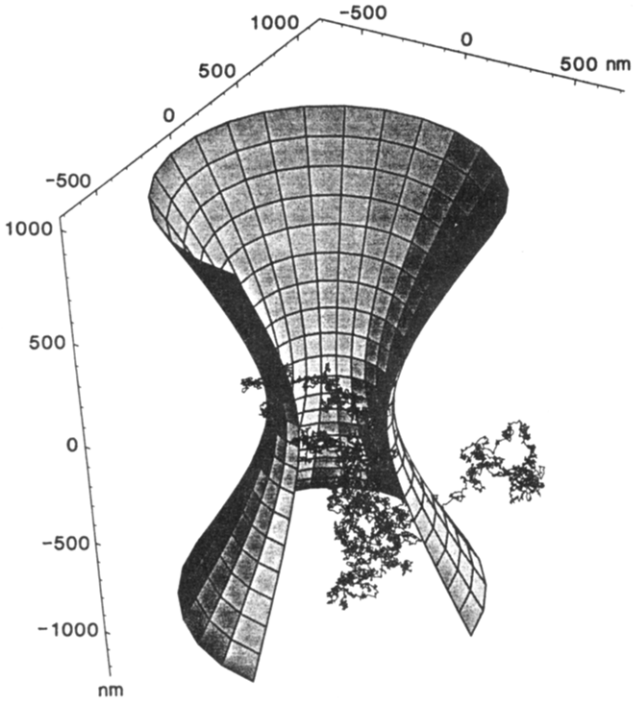

Figure 5. diffusion path of a single R6G molecule in a 1-ms period in solution at room temperature. The conical drawing represents the $1/e^2$ boundary of the tightly focused laser beam and is cut open to show the molecule's path as marked by the dark, wiggly line. Simulation parameters: starting position of the molecule, center of the conical laser beam; incremental step (Δt), 0.1 μs; laser beam radius, 260 nm; R6G diffusion coefficient, 2.8×10^{-6} cm^2 s^{-1}.

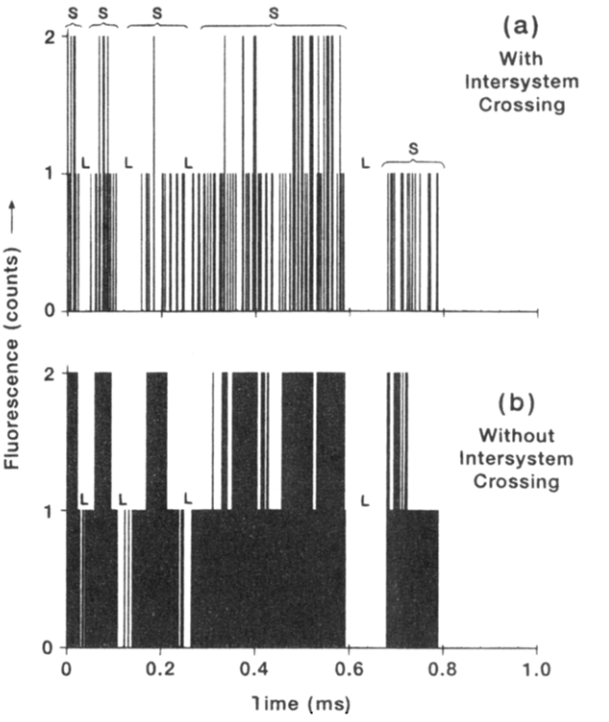

Figure 6. Simulated fluorescence records of single R6G molecules in the presence (a) and the absence (b) of the long-lived triplet state in a 1-ms period in solution. We label by L the long gaps caused by boundary recrossing and by S the short gaps caused by intersystem crossing. Simulation parameters: starting position of the molecule, center of the conical laser beam; incremental step (Δt), 0.1 μs; integration time per data point, 2 μs; laser wavelength, 514.5 nm; excitation power, 1 mW; laser beam radius, 260 nm; R6G diffusion coefficient, 2.8×10^{-6} cm^2 s^{-1}; R6G extinction coefficient at laser wavelength, 5.8×10^4 M^{-1} cm^{-1}; combined photon detection efficiency, 0.9%; triplet-state lifetime, 4 μs; singlet-state lifetime, 3.4 ns; intersystem crossing efficiency, 0.2%.

molecule in solution during a 1-ms period. The path, as marked by the wiggly line, contains several excursions into and out of the probe volume boundary, corresponding to the long dark gaps in the simulated fluorescence records shown in Figure 6. The average duration (~50 μs) of such simulated dark gaps qualitatively agrees with the experimental data. The simulation also shows the appearance of short dark gaps if the triplet state is included but only the long dark gaps if the triplet state is ignored. It thus appears that intersystem crossing into and out of the long-lived triplet state is mainly responsible for causing the short dark periods in our real-time measurements.

Rigler and co-workers[22,23,25-27] also studied the diffusion and triplet-state involvement for R6G molecules with fluorescence correlation analysis and a similar experimental setup. They found that the triplet-state buildup at high excitation intensities causes a distortion in the autocorrelation curve. Major differences appear between the fluorescence correlation data and the real-time measurements of this work, however, especially in the diffusional motions of single molecules. The individually measured transit times for R6G are in the range of 0.5–1.2 ms (0.7 ms typical), which are 10–30 times longer than those (40–50 μs) reported by Rigler and co-workers under similar conditions.[22] This difference may be reconciled by noting that real-time fluorescence measurements are biased toward molecules that spend longer periods of time in the probe volume and that the detection events are dominated by molecules that have long paths in the probe volume. The diffusion times of these molecules may be approximately estimated by the time (~0.5 ms) the molecules take to traverse the laser beam diameter (not the radius) because a single molecule must first enter and then exit the probe volume in real-time measurements. On the other hand, the characteristic autocorrelation time is usually dominated by the fastest signal fluctuations,[28] such as those caused by recrossings into and out of the triplet state and the probe volume periphery. Therefore, the diffusion times measured by fluorescence correlation are likely to correspond to boundary recrossing motions and not the global, traversing motions observed in real-time measurements. As discussed above, the boundary recrossing motions of single R6G molecules occur on the time scale of ~50 μs, consistent with reported correlation times (40–50 μs).

For fluorescent dyes of low intersystem crossing yields and high photostabilities, a single molecule can produce 300–400 detected photons during a 1-ms transit time across the probe volume. Thus, detection of a single molecule is possible with a signal-to-noise ratio of ~20 in only 1 ms under shot-noise-limited conditions. The results presented show that the detection sensitivity in confocal fluorescence microscopy can indeed be optimized to approach the theoretical limit for R6G molecules, even though the subfemtoliter-sized probe volume still contains

(55) The simulation was based on the Einstein equation of Brownian motion as described by Chandrasekhar and was implemented by using a numerical procedure; see: Chandrasekhar, S. *Rev. Mod. Phys.* **1943**, *15*, 20. Press, W. H.; Flannery, B. P.; Teukolsky, S. A.; Vetterling, W. T. In *Numerical Recipes: The Art of Scientific Computing*; Cambridge University Press: New York, 1986; p 202.

$\sim 1.5 \times 10^{10}$ solvent molecules, $\sim 5 \times 10^{7}$ electrolyte molecules, and many impurity molecules. A key factor is that the unlimited excitation throughput allows fluorescence photons to be extracted from a single molecule at the maximum (saturation) speed for fluorescence cycling. Another factor is the relatively low background level (~2–6 counts/ms) as compared with the typical fluorescence signals (~100–150 counts/ms). Under these shot-noise-limited conditions, our results show that single R6G molecules are detected with a signal-to-noise (peak-to-peak) ratio of ~10 with 1-ms integration. This detection sensitivity is only a factor of 2 below the theoretical limit, which is set by fluorescence saturation in this case. It also compares favorably with that achieved in near-field optical microscopy, which breaks the diffraction limit by confining the light source to nanometer dimensions.[44,45] Despite the dramatically reduced probe volume (attoliters or 10^{-18} L) in the near-field, the reported background level (2 counts/ms)[43] is not significantly lower than that of this work (2–6 counts/ms).

Biomolecules. Previous studies in single-molecule detection and spectroscopy have focused mainly on simple fluorescent dye molecules, except perhaps fluorescence correlation studies of rhodamine-labeled M13 DNA, BODIPY-labeled primers, and rhodamine-labeled bungarotoxin–acetylcholine receptor conjugates.[27] By capitalizing on the extraordinary sensitivity achieved with confocal fluorescence microscopy, we demonstrate real-time detection of individual, fluorescently labeled biomolecules in buffer solution. The labeled molecules retain their biological functions if the labels are attached appropriately, such as through a linker arm.[56,57] Figure 7 shows detection of individual deoxyuridine triphosphate molecules labeled with fluorescein via a 12-atom linker arm (fluorescein-12–dUTP) in aqueous solution containing 2-mercaptoethanol (~100 mM). Fluorescein-12–dUTP is widely used for nonradioactive labeling of DNA and is a suitable substrate for *Escherichia coli* DNA polymerase I, T4 DNA polymerase, Taq DNA polymerase, and reverse transcriptase.[58] This modified nucleotide can be substituted for dTTP in nick-translation reactions and the fluorescence-labeled probes are used in fluorescence in situ hybridization. As for free fluorescein, the fluorescence efficiency of the tagged nucleotide is strongly enhanced at basic pH and by the presence of an antibleaching agent such as mercaptoethanol. This behavior is apparently explained by the sensitive nature of fluorescein to pH and by its photobleaching properties in aqueous environments. In contrast, rhodamine dyes are insensitive to pH and highly photostable. Indeed, the fluorescence signals of the same nucleotide labeled with TMR show little dependence on solution pH or on the presence of antibleaching agents. By using a weighted quadratic summing filter, Soper et al.[31] also showed fluorescence detection of single adenine nucleotides labeled with TMR in a flowing stream. Photobleaching does not appear to be a significant factor during the ~1-ms measurement time for fluorescein-labeled nucleotide with mercaptoethanol protection and for rhodamine-labeled molecules without protection, as evidenced by the similar fluorescence intensities detected for molecules of greatly different photodestruction efficiencies. Compared with free fluorescein, fluorescein-12–dUTP has a lower diffusion coefficient and is thus expected to have a longer diffusion time across the probe volume. Indeed, the fluorescence signals (~60 counts) of fluorescein-12–dUTP are higher than those of fluorescein (~50 counts). A complicating factor, however, is that the fluorescent properties of fluorescein may change upon conjugation to dUTP via the 12-atom linker.

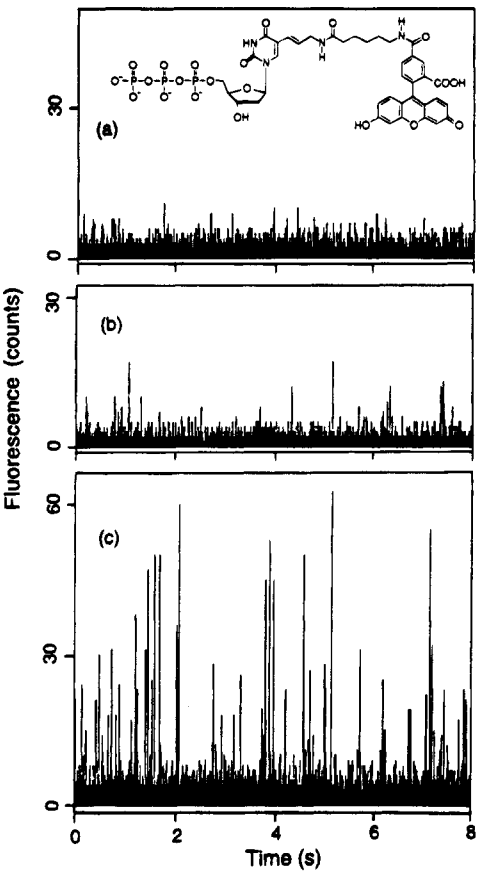

Figure 7. Detection of individual deoxyuridine triphosphate molecules labeled with fluorescein via a 12-atom linker arm (fluorescein-12–dUTP) in aqueous 100 mM mercaptoethanol solution: (a) blank; (b) 2×10^{-10} M fluorescein-12–dUTP at pH 7.0; (c) 2×10^{-10} M fluorescein-12–dUTP at pH 12. Laser wavelength, 488 nm; excitation power, 0.2 mW; emission bandpass filter, 530 nm (fwhm 60 nm); integration time per data point, 1.0 ms.

Fluorescence signals have also been observed from individual M13/pUC primers labeled at the 5′ end with fluorescein and BODIPY FL in Tris buffer. This primer is a single-stranded oligonucleotide, d(TGAAAACGACGGCCAGT), and is useful for automated sequencing of DNA fragments cloned into the M13 mp vector series and pUC or pUC-related plasmid.[59] BODIPY FL is similar to fluorescein in its extinction coefficient (>80 000 cm^{-1} M^{-1}) and quantum yield (close to unity). It may be considered superior to fluorescein because of its remarkable insensitivity to solvent pH, improved photostability, reduced fluorescence quenching when conjugated to proteins or oligonucleotides, and narrower emission bandwidth.[60] However, the

(56) Zhu, Z.; Chao, J.; Yu, H.; Waggoner, A. S. *Nucleic Acids Res.* **1994**, *22*, 3418–3422.
(57) Leary, J. J.; Brigati, D. J.; Ward, D. C. *Proc. Natl. Acad. Sci. U.S.A.* **1983**, *80*, 4045–4049. Langer, P. R.; Waldrop, A. A.; Ward, D. C. *Proc. Natl. Acad. Sci. U.S.A.* **1981**, *78*, 6633–6637.
(58) Dirks, R. W.; Van Gijlswijk, R. P. M.; Vooijs, M. A.; Smit, A. B.; Bogerd, J.; Van Minnen, J.; Raap, A. K.; Van Der Ploeg, M. *Exp. Cell Res.* **1991**, *194*, 310–315.
(59) Messing, J. *Methods Enzymol.* **1983**, *101*, 20–78.
(60) Haugland, R. P. *Handbook of Fluorescent Probes and Research Chemicals*, 5th ed.; Molecular Probes: Eugene, OR, 1994.

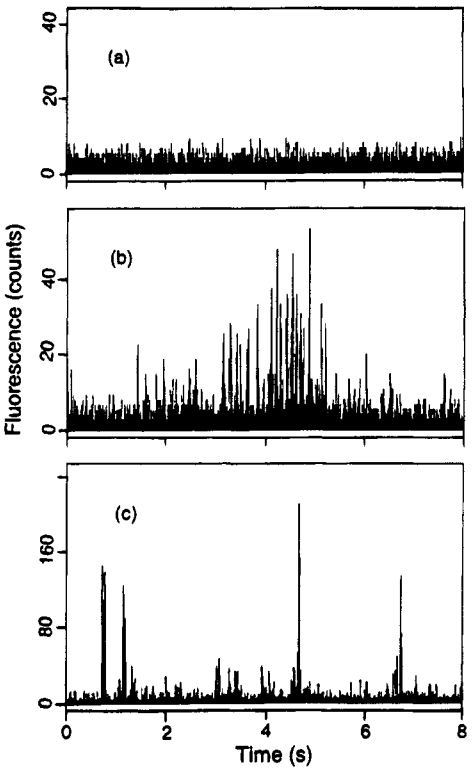

Figure 8. Real-time observation of λ-phage DNA (48 502 bp) structural fluctuations in free solution (TBE buffer pH 8): (a) background from unlabeled DNA in TBE buffer; (b) fluorescence signals from a λ-DNA molecule labeled with the bis-intercalating fluorescent dye YOYO; (c) 14-nm fluorescent microspheres. Laser wavelength, 488 nm; excitation power, 0.4 mW; emission bandpass filter, 530 nm (fwhm 40 nm); integration time per data point, 1.0 ms.

fluorescence signals obtained from single molecules of the BODIPY-labeled primer are slightly weaker than those of fluorescein-labeled primers. The number of photons obtained from a single molecule is determined by the fluorescence cycle rate and is ultimately limited by photobleaching. This result seems to indicate that BODIPY has a lower fluorescence cycle rate (caused by a longer triplet lifetime or a higher intersystem crossing efficiency).

Figure 8 depicts fluorescence signals observed from a single λ-phage DNA molecule (48.5 kbp) labeled with YOYO in TBE buffer, along with data from 14-nm fluorescent microspheres for comparison. The bis-intercalating asymmetric cyanine dye YOYO shows an extremely high affinity for nucleic acids and a more than 1000-fold fluorescence enhancement upon binding to double-stranded DNA.[46,47] Unlike the simple fluorescence signals observed from individual microspheres and small molecules, each detection event of a λ-DNA molecule consists of a series of fluctuating signals with temporal spacings of 10−100 ms. This complex behavior is apparently caused by dynamic structural changes of the DNA molecule, because no such fluctuations were seen for polymeric microbeads of various sizes (14 nm to 1.0 μm in diameter) that lack internal structures. Although the number of intercalated dye molecules per DNA molecule is not accurately known, the low dye/DNA molar ratio ensures that each DNA molecule contains only a small number of fluorescent tags. The probe volume then would contain no more than a few or a single tag. DNA internal motions repeatedly bring these fluorescent dyes into and out of the field of view, which results in fluorescence signal fluctuations. Such large-amplitude motions may be caused by the elasticity and flexibility of the DNA chain and intramolecular forces (i.e., superhelical formation). We further note that the observed signal fluctuations last considerably (~25 times) longer than the estimated transit time.[61] This unusual persistence time may be caused by an optical trapping effect,[62] attachment of DNA molecules to the glass coverslip surface, or multiple recrossings of the probe volume by a single DNA molecule.

The observed DNA shape and structural fluctuations make for interesting comparison with those reported in the literature. Real-time observation of individual DNA molecules labeled with numerous fluorescent dyes have been achieved in confined media,[63−66] in free solution,[67−70] and through attachment to magnetic[71,72] and dielectric microbeads.[73] In electrophoresis gels or entangled solution, DNA molecules are shown to snake their way through the restricted media in an extended configuration and alternatively contract and lengthen as they move. They often become hooked around obstacles in a U shape for extended periods and show an elastic behavior.[63−66] In free solution, DNA molecules stained with 4′,6-diamindino-2-phenylindole (DAPI) show thin and extended filaments, thick and short filaments, and rapidly changing spherical and ellipsoidal structures.[67] The thick filaments are very flexible, swaying and exhibiting waves of irregular length, and they frequently extend and contract. The DNA structural fluctuations observed in this work appear consistent with these studies, but they occur on considerably shorter time scales than those reported previously. Apparently, the present study's use of a submicrometer-sized laser beam selectively probes local internal motions of a DNA molecule, whereas previous studies mainly detect global DNA movements. Further insights may be obtained by studying DNA molecules that are fluorescently labeled at one end and attached to a surface at the other.

In summary, we have demonstrated that confocal fluorescence microscopy provides a simple and sensitive means for real-time observation of single fluorescent molecules in solution. Because of the unlimited excitation throughput and low background level, the achieved detection sensitivity for single R6G molecules is only a factor of 2 below the theoretical limit. Real-time measurements at a data acquisition speed of 500 kHz show single-molecule fluorescence records with a time spread that corresponds to the actual transit time of a particular molecule. The obtained fluorescence records consist of predominantly single-photon events and contain both long (~50 μs) and short (~4 μs) dark gaps. Simulation studies of single fluorescent molecules provide evidence that these long and short dark periods are caused mainly by boundary recrossing motions of a single molecule at the probe

(61) The diffusion coefficient of λ-phage DNA (48 502 bp) in dilute aqueous solution has been measured to be 4.2 (±2) × 10^{-9} cm^2 s^{-1} by fluorescence correlation spectroscopy; see: Scalettar, B. A.; Hearst, J. E.; Klein, M. P. *Macromolecules* **1989**, *22*, 4550−4559.

(62) Chu, S. *Science* **1991**, 253, 861−866. Chu, S. *Sci. Am.* **1992**, (Feb), 71−76.
(63) Smith, S. B.; Aldridge, P. K.; Callis, L. B. *Science* **1989**, *243*, 203−206.
(64) Schwartz, D. C.; Koval, M. *Nature* **1989**, *338*, 520−522.
(65) Rampino, N. J.; Chrambach, A. *Anal. Biochem.* **1991**, *194*, 278−283.
(66) Volmuth, W. D.; Austin, R. H. *Nature* **1992**, *358*, 600−602.
(67) Yanagida, M.; Hiraoka, Y.; Katsura, I. *Cold Spring Harbor Symp. Quant. Biol.* **1983**, *47*, 177−187.
(68) Morikawa, K.; Yanagida, M. *J. Biochem.* **1981**, *89*, 693−696.
(69) Matsumoto, S.; Morikawa, K.; Yanagida, M. *J. Mol. Biol.* **1981**, *152*, 501−516.
(70) Song L.; Maestre, M. F. *J. Biomol. Struct. Dynam.* **1991**, *9*, 525−536.
(71) Smith, B. S.; Finzi, L.; Bustamante, C. *Science* **1992**, *258*, 1122−1126.
(72) Bustamante, C. *Annu. Rev. Biophys. Biophys. Chem.* **1991**, *20*, 415−446.
(73) Perkins, T.; Smith, D. E.; Chu, S. *Science* **1994**, *264*, 819−822. Perkins, T.; Quake, S. R.; Smith, D. E.; Chu, S. *Science* **1994**, *264*, 822−826.

volume periphery and by intersystem crossing into the dark triplet state. We have also extended the use of confocal fluorescence microscopy to study individual biological molecules in buffer solution. Through fluorescent labeling, single-molecule detection has been achieved for deoxynucleotides, oligonucleotides, and double-stranded DNA molecules. The extraordinary sensitivity allows structural dynamics studies of individual DNA molecules labeled with only a few or a single fluorescent tag. The results show that λ-phage DNA in free solution undergoes large-amplitude structural fluctuations that repeatedly bring the fluorescent labels into and out of the probe volume.

ACKNOWLEDGMENT

S. N. acknowledges the Whitaker Foundation for a young investigator award. D.T.C. is a Beckman Cell Science Scholar of Stanford University. This work was supported by Beckman Instruments, Inc.

Received for review February 15, 1995. Accepted June 5, 1995.[⊗]

AC950164B

[⊗] Abstract published in *Advance ACS Abstracts,* July 1, 1995.